A stepwise kinetic approach to quantify rate coefficients for reactant-, auto- and non-catalyzed urethanization of phenyl isocyanate and 1-butanol

Lynn Trossaert [a,b], Mariya Edeleva [b], Paul H. M. Van Steenberge [a], Hendrik Kattner [c] and Dagmar R. D'hooge [a,d*]

[a.] *Laboratory for Chemical Technology (LCT), Ghent University, Technologiepark 125, B-9052 Gent, Belgium. E-mail: dagmar.dhooge@ugent.be*
[b.] *Centre for Polymer and Material Technologies (CPMT), Ghent University, Technologiepark 130, B-9052 Gent, Belgium.*
[c.] *BASF SE, Carl-Bosch-Strasse 38, Ludwigshafen am Rhein 67056, Germany.*
[d.] *Centre for Textile Science and Engineering (CTSE), Ghent University, Technologiepark 70a, B-9052 Gent, Belgium.*

Limited kinetic information is available on the formation of polyurethanes with still unclarity on the exact reaction mechanism, which is complicated by the less understood competition between non-catalyzed and molecule-assisted reactions such as catalysis by the alcohol, the isocyanate, and the carbamate. In the present work, focusing on urethane formation based on the monofunctional analogues 1-butanol and phenyl isocyanate in dichloromethane, a two-step kinetic approach is presented that is capable to first deliver rate coefficients and Arrhenius parameters as expected relevant under diluted conditions, to then determine rate coefficients of extra reactions as likely most relevant in large excess of one of the reactants. More in detail, gas chromatography and UV-Vis analysis have been applied to quantify (carbamate) product yields as a function of time under quasi stoichiometric concentrations and with a large 1-butanol excess, and reaction-event driven kinetic Monte Carlo modeling is applied to tune the rate coefficients at a given temperature. It is shown that butanol catalyzed and carbamate catalyzed reactions are the most activated, and the formation of a complex based on two 1-butanol molecules and 1 phenyl isocyanate molecule has a significant influence on the kinetics, which comes only measurable in case of high initial alcohol concentrations. The kinetic interpretations are supported by reaction probability variations as well as sensitivity analyses. The present two-step kinetic approach opens the door to deliver more reliable elementary-driven rate coefficients for (poly)urethane systems and showcases that even under conventional conditions as relevant for at least solution polyurethane formation unconventional complex-based mechanisms can be more active than we currently anticipate based on conventional kinetic laws.

Introduction

Since the discovery of polyurethane (PU) in 1937, [1, 2] this step-growth polymer has gained growing commercial importance. Already in the 1940s, this material was used for millable elastomers, coatings, adhesives and fibers, while starting from the 1960s the use of PU was extended to flexible and rigid foams. [3] Through alternation of the PU molecular structure, a large range of properties can be obtained, [4, 5] with variations in average molar mass, intermolecular forces, chain stiffness, crystallization potential, and degree of crosslinking within reach. [1, 6-8] These variations make PU suitable for a broad span of products, from footwear and clothing to furniture and bedding, to construction and the automotive industry.[4, 9, 10] Because of this versatility, PU is one of the most produced polymers worldwide, [11] competing with some commodity and specialty chain growth polymers, [12] with an expected production of 22.5 million tons by 2024. [13]

Chemically, PU molecules are the main reaction products of the step-growth polymerization between molecules containing isocyanates (-N=C=O) and active hydrogens, i.e., alcohols. In the most simple reaction scheme as shown in Scheme 1a,[1, 14] urethane linkages are directly formed in one step, with the commonly used diisocyanates in the PU industry being 4,4-methylene diphenyl diisocyanate (4-4'-MDI) and toluene diisocyanate (both 2,6-TDI and 2,4-TDI), as highlighted in Scheme 1b,[5, 6] and the most used polyols being polyether- and polyester-polyols.[15] Specifically, in applications requiring more rigid materials shorter polyols are employed [6]. Depending on the functionality of the alcohol, the resulting polymer can be linear, branched or crosslinked as well.[3, 16]

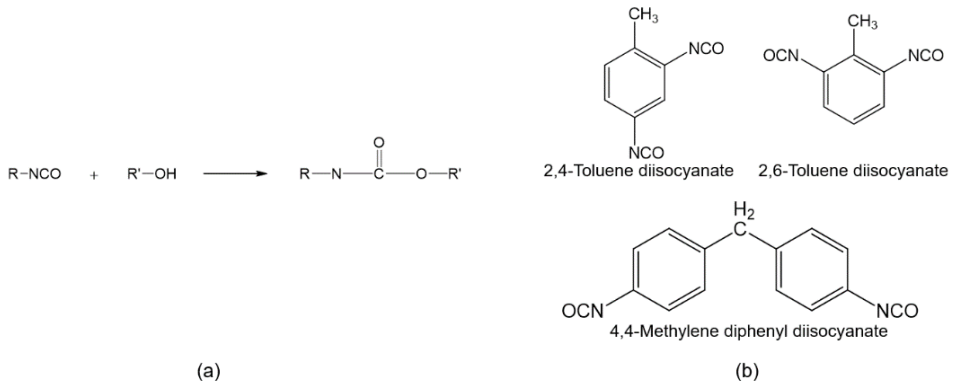

Scheme 1: (a) (Apparent) reaction between an isocyanate and an alcohol to form a urethane group; (b) Selected commercially relevant diisocyanates.

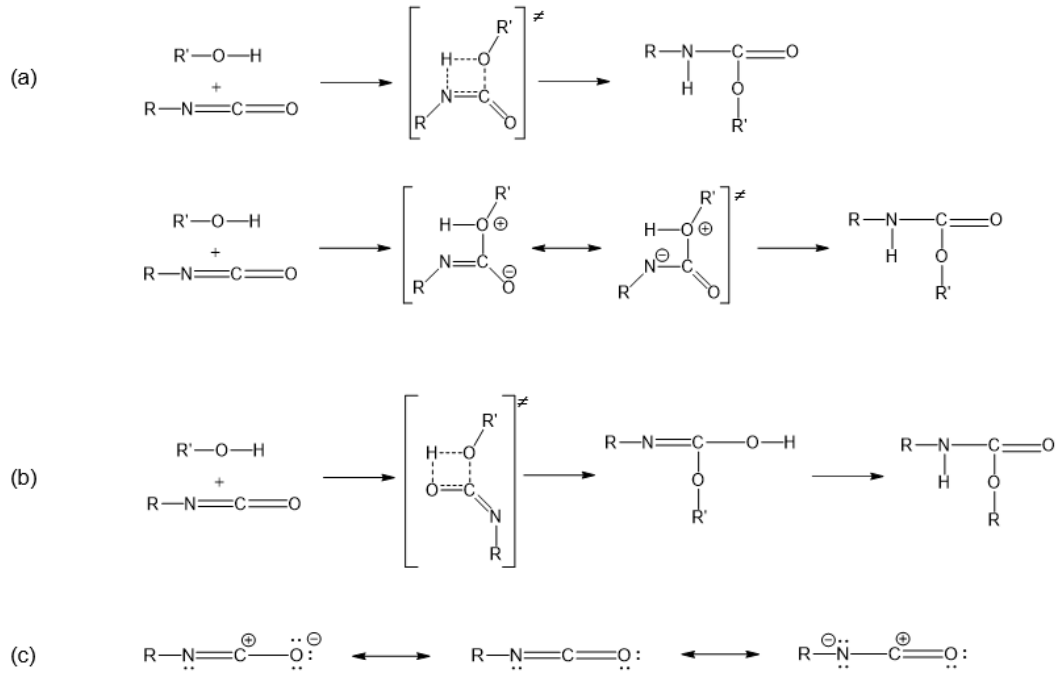

Scheme 2: Non-catalyzed mechanisms: (a) 1 step mechanism, (b) 2 step mechanism, (c) Resonance structure leading to a positive charge on the isocyanate carbon.

According to the one-step mechanism, as shown with several transition states in Scheme 2a, the isocyanate (R-NCO) reacts by addition of the proton-bearing nucleophile, as exemplified by the alcohol molecule R'-O-H, to the carbon-nitrogen double bond. The active hydrogen becomes attached to the isocyanate nitrogen, while the OR' group binds covalently to the carbon atom. Also a two-step mechanism has been proposed, as highlighted in Scheme 2b, [1, 5, 14, 17] in which the hydrogen of the alcohol interacts with the oxygen of the isocyanate. In any case, the urethane formation is enhanced by the resonance structure for the isocyanate, allowing a partially positive charge on the carbon atom and a partially negative charge on the nitrogen or oxygen atom, as highlighted in Scheme 2c. [5, 6]

The molecular structure of the isocyanate and nucleophile have a significant influence on the rate of the urethane formation. Secondary and tertiary alcohols react 0.3 and 0.005 times slower than primary alcohols at 298-323 K, respectively. [1, 18, 19] In general, isocyanates are known to be very reactive toward proton-bearing nucleophiles, which, in addition to alcohols, include amines, urea, carboxylic acids and even urethanes. Isocyanates containing electron-withdrawing groups such as aromatic moieties react faster than aliphatic ones. The presence of an electron-withdrawing group stabilizes the partially positive charge on the carbon,[6] facilitating the proton shift from the O- to the N-atom.[1] Furthermore, the reaction between an isocyanate moiety and a hydroxyl group is already rather fast at room temperature. [1, 6] It has been indicated that temperatures above 383 K should

preferably be avoided for achieving a linear macromolecular structure, since side reactions might become too relevant.[6] Allophanate linkages via coupling of isocyanate and urethane moieties, and biuret linkages via coupling of isocyanate and urea linkages, significantly increase the crosslinking density, as highlighted in Scheme 3a.[6, 9]
Even at low temperatures, side products can be observed in the presence of water being the simplest form of a hydroxy-active compound. A carbamic acid is first formed by the reaction of water with an NCO group, as shown in Scheme 3b, which decomposes because of its rather instability into an amine under CO_2 release. The gas formed can lead to foam production, while the amine is usually consumed by free isocyanate forming urea groups, as also depicted in Scheme 3b.[1, 3, 9, 20] Other side reactions are the dimerization and trimerization of isocyanate, as highlighted in Scheme 3c, which can occur spontaneously and is further promoted by catalysts.[6] Trimers formed through this type of side reaction are often quite stable, contrary to the dimers. Moreover, aromatic isocyanates have shown to be more prone to form these ring structures.[21]
Despite that PU is produced annually in large amounts, still no consensus about the exact reaction mechanism exists. The conventional (non-catalyzed) isocyanate-alcohol coupling described in Scheme 2a-b is very likely not the only reaction path, since in many cases urethane formation cannot be described by first order kinetics in each reactant. Instead, variations in reaction order have been detected by several authors.[5, 22-28] It is thus not surprising that multiple reaction pathways have been proposed, deviating from an overall second order reaction. The most important schemes, with examples in Scheme 4, rely on catalytic (or molecule-assisted) pathways induced by (one of the) reagents or the product, which are commonly denoted as alcohol catalysis, isocyanate catalysis and carbamate catalysis.[5, 9, 10, 14, 22-27, 29-33] In Scheme 4 and in subsequent schemes, species presented between brackets represent (isolated) complexes, and the symbol ≠ represents a transition state.

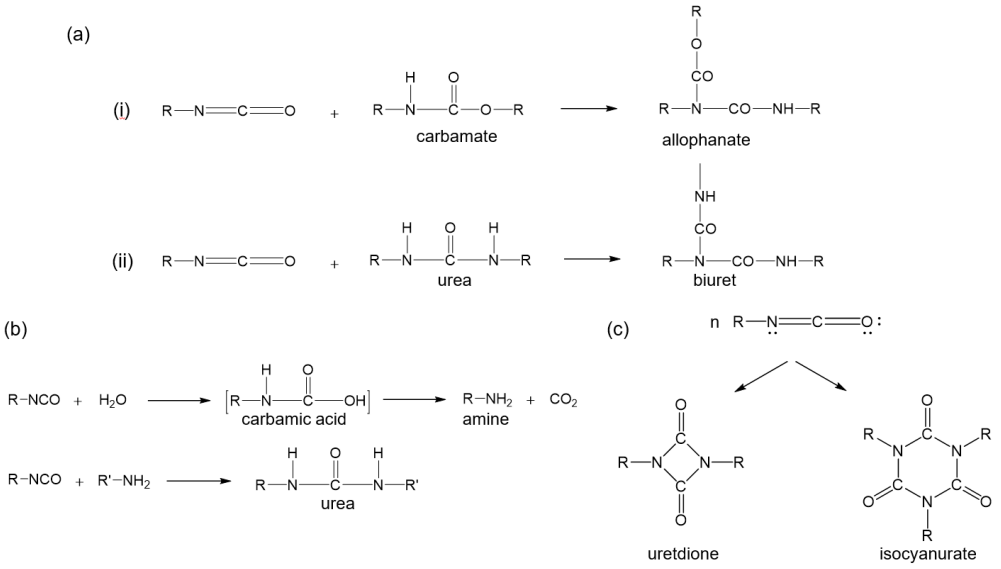

Scheme 3: Side reactions for urethane formation: (a) Allophanate (i) and biuret (ii) crosslink; (b) Side reaction with water resulting in the formation of gas and urea; (c) Dimerization and trimerization of isocyanate.

The urethane formation can be catalyzed by acidic and basic catalysts, including amines and metal-organic, in particular tin-organic compounds. However, the latter compounds are not preferred because of their toxicity.[2, 9, 17, 34] Base catalyzed PU formation can take place by activating the alcohol (example of alcohol catalysis; Scheme 4a), whereas an example of an acid catalyst for isocyanate catalysis is given in Scheme 4b, activating the isocyanate. Organotin compounds follow a similar path as the acids [17, 24]. Eceiza et al. [5] confirmed the base catalyzed reaction for alcohol catalysis, proposing that Lewis bases can increase the nucleophilic properties by raising the partial negative charge of the alcohol oxygen. Even in the absence of a (deliberately added) catalyst, a second alcohol molecule can behave as a Lewis base or "nucleophilic activator", as shown in Scheme 4c. This (alcohol) molecule-assisted mechanism was proposed by Baker et al.,[31] whose research in 1948 already confirmed that the reaction rate for the urethane formation is dependent on the initial alcohol concentration. Similar reports have been highlighting the catalytic (or molecule assisted) effect of the urethane group.[5, 22, 25, 33] This autocatalytic pathway can be treated as intrinsic for urethane formation, similar to the alcohol catalysis. For example, the carbamate autocatalysis mechanism proposed by Eceiza et al.[5] for (Scheme 4d) is similar to the one in Scheme 4c, describing the alcohol catalysis. While Eceiza et al.[5] describe a complex formation between a

urethane and an isocyanate molecule, Samuilov et al.[33] put forward that the carbamate can undergo H-bonding with the alcohol. This interaction enhances the nucleophilicity of the hydroxyl group even more than the alcohol association in the alcohol catalysis.

Since associates of isocyanates can be formed due to their large electric dipole moment, additional reaction pathways can be assumed. For example, Cheikh et al.[32] proposed a mechanism in which a urethane linkage is formed starting from a six centered ring containing one alcohol and two isocyanate molecules to form an allophanate molecule that is rearranged with isocyanate release, as displayed in Scheme 4e. Consistently, the experimental results of Cheikh et al.[32] could confirm an increase in the apparent rate coefficient under isocyanate excess. Furthermore, in the computational chemistry part of Cheikh et al.[32], hydrogen bonding stabilized alcohol associates have been put forward, as based on complex formation involving one isocyanate and two alcohols. The proposed mechanism is shown in Scheme 5a and consists of a six centered transition state. The catalytic effect was confirmed by experiments between 1-propanol and phenyl isocyanate. Complementary, Gertig et al.[14] described both a six centered and eight centered ring structure transition state in their computational study, as shown in Scheme 5b. For higher alcohol concentrations and in non-polar solvents, the eight centered ring was claimed as the most important one, having the most favorable energy, while for lower excesses of alcohol and in polar solvents both transition states were claimed to exist, since it requires more energy to break the bonds that are formed between the alcohol and the solvent. In general, a very complex reaction scheme with several competitive reaction pathways (cf. Scheme 1-5) can thus be formulated for PU synthesis and even for the urethane formation with limited chain growth as based on monofunctional species. As shown in the present work, for the monofunctional compounds phenyl isocyanate PhNCO and 1-butanol (Scheme 6) already a handful rate coefficients are required to describe the kinetics over a broad range of initial conditions. Consequently, the experimental determination of PU rate coefficients requires both accurate kinetic measurements and sophisticated, model-driven data processing.

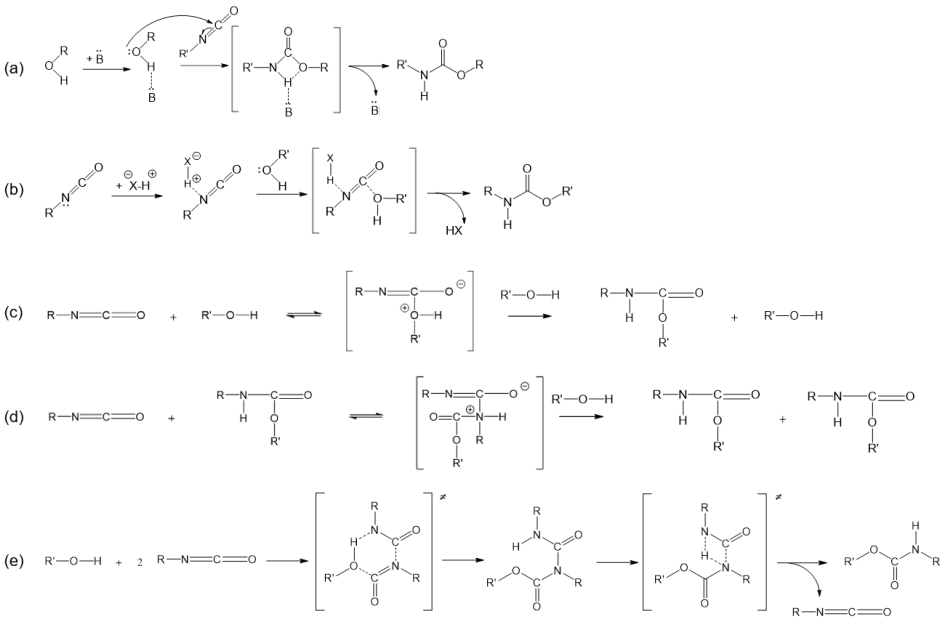

Scheme 4: Proposed mechanisms to catalyze the urethane formation: (a) Activation of the alcohol by a Lewis base [2]; (b) Activation of the isocyanate by a Lewis acid; [2] (c) catalysis by the alcohol of the urethane formation reaction according to Baker et al. including the formation of an intermediate; [31] (d) Autocatalysis by the urethane described by Eceiza et al. including the formation of an intermediate;[5, 10] (e) Isocyanate catalysis mechanism according to Cheikh et al.[32]

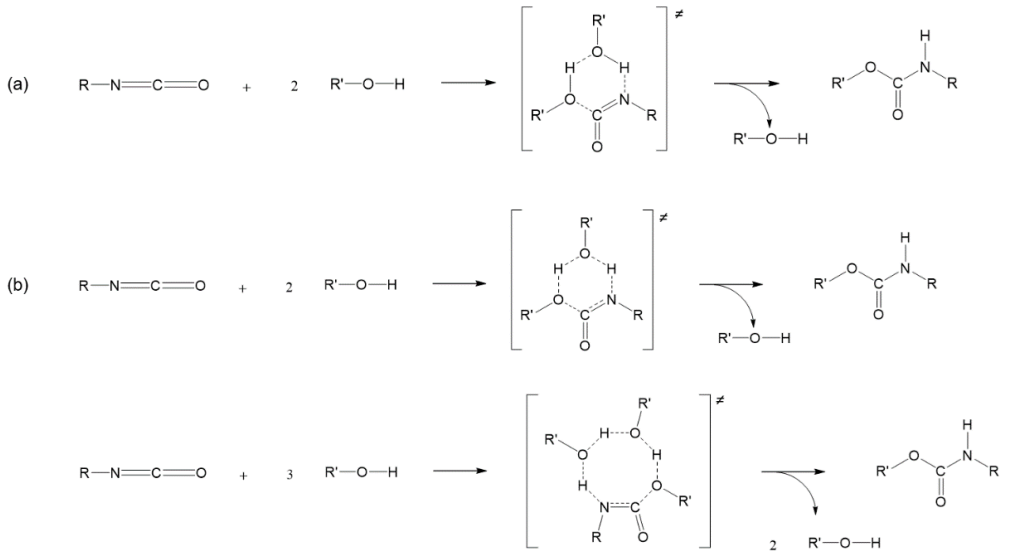

Scheme 5: Additional alcohol catalysis mechanism (cf. Scheme 4) proposed by (a) Cheikh et al.[32] and (b) Gertig et al.[14]

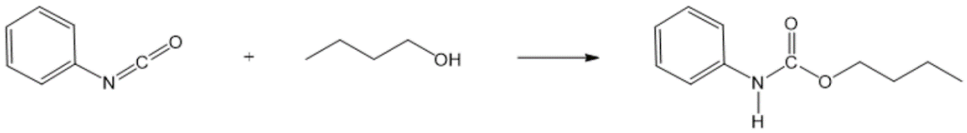

Scheme 6: Reaction between phenyl isocyanate and 1-butanol toward butyl phenyl carbamate, as the monofunctional analogue for PU formation, studied in the present work.

Table 1: Summary of effective thus apparent/observed rate coefficients and effective thus apparent activation energies for the reaction between an alcohol and an isocyanate, as found in literature. PhNCO: phenyl isocyanate; MDI: 4,4-methyl diphenyl diisocyanate; HDI: 1, 6-hexamethylene diisocyanate; PHMC-co-PCL: poly(hexamethylene carbonate-co-caprolactone)diol; THF: tetrahydrofuran; EVHOSO-AA: epoxidized fatty acid methyl ester of very high oleic sunflower oil (EVHOSO) ring-opened with acetic acid.

Isocyanate	**Alcohol**	**Solvent**	***T [K]***	**Kinetic parameters**	**Reference**
PhNCO	1-butanol	toluene	298	k_{eff} = (2 – 4) 10^{-4} L mol^{-1} s^{-1}	24
PhNCO	1-butanol	chlorobenzene	318	k_{eff} = 1.17 10^{-2} L mol^{-1} s^{-1}	35
PhNCO	1,4-dibutanol	1,4-dioxane	308	k_{eff} = 0.54 10^{-4} L mol^{-1} s^{-1}	35
MDI	1-butanol	toluene		*Ea,eff = 20 kJ mol-1* *Ea,eff = 20.5 ± 2.8 kJ mol-1*	30
PhNCO	1-butanol	cyclohexane	298	k_{eff} = 3.9 10^{-2} L mol^{-1} s^{-1}	6
PhNCO	1-butanol	chlorobenzene	298	k_{eff} = 8.0 10^{-3} L mol^{-1} s^{-1}	6
PhNCO	1-butanol	benzene	298	k_{eff} = 5.8 10^{-3} L mol^{-1} s^{-1}	6
PhNCO	1-butanol	nitrobenzene	298	k_{eff} = 1.8 10^{-3} L mol^{-1} s^{-1}	6
PhNCO	1-butanol	ethyl acetate	298	k_{eff} = 0.18 10^{-3} L mol^{-1} s^{-1}	6
PhNCO	1-butanol	acetonitrile	298	k_{eff} = 0.15 10^{-3} L mol^{-1} s^{-1}	6
PhNCO	1-butanol	dioxane	298	k_{eff} = 0.80 10^{-2} L mol^{-1} s^{-1}	6

HDI	PHMC-co-PCL	-		Non-catalytic reaction; Ea = 43.5 ± 1.5 kJ mol-1 A = 1.9 10_4 L mol^{-1} s^{-1} Autocatalytic reaction; Ea = 90 ± 2.5 kJ mol-1 A = 4.2 10_{10} L mol^{-1} s^{-1}	[29]
PhNCO	1-butanol	chlorobenzene	303	k_{eff} = 1.51 10^{-4} L mol^{-1} s^{-1} Non-catalytic reaction; k = 2.32 10^{-5} L mol^{-1} s^{-1} Ea = 31 kJ mol-1 Autocatalytic reaction; k = 9.18 10^{-4} L mol^{-1} s^{-1} Ea = 19 kJ mol-1	[33]
PhNCO	1- butanol	toluene	293	k_{eff} = 82 10^{-4} L mol^{-1} s^{-1}	[26]
PhNCO	1- butanol	methyl ethyl ketone	293	k_{eff} = 3.0 10^{-4} L mol^{-1} s^{-1}	[26]
PhNCO	1-propanol	THF		With alcohol excess; Ea,eff = 30.4 ± 1.6 kJ mol-1 Aeff = 18.8 ± 1.0 L mol-1 s-1 Stoichiometric conditions; $E_{a,eff}$ = 58.6 ± 6.0 kJ mol^{-1} A_{eff}= (2.34 ± 0.24) 10_5 L mol^{-1} s^{-1} With isocyanate excess; $E_{a,eff}$ = 44.2 ± 4.5 kJ mol^{-1} A_{eff} = (2.15 ± 0.22) 10_2 L mol^{-1} s^{-1}	[32]
PhNCO	EVHOSO-AA	toluene	298	*keff = 1.7 10-5 L mol-1 s-1*	[36]

Many kinetic studies, despite their quantitative pretensions, tend to neglect the (auto-)catalytic reactions and to perform simplifications. For example, Huang et al. [22] determined in their model the rate coefficient of the reaction between 1,5-naphtyl diisocyanate and 1-butanol, assuming pseudo first order kinetics of the isocyanate. Deviations of the model output compared to experimental data at high conversions were explained by the autocatalytic effect of the urethane group, without accounting for this reaction in an updated model. Another example of a typical kinetic model is that of Krol[37] considering experimental data for the reaction between 2,4-toluene diisocyanate and 1,4-butanediol. Overall second order kinetics were assumed, and the model consisted of a set of differential and algebraic equations. (Auto)-catalytic effects were, however, not taken into account. Other kinetic modeling studies[38-40] described the gel effect during PU formation by assuming second order kinetics as such. Catalytic effects were neglected, leading to non-optimal modeling results.
In Table 1, a summary is made of apparent rate coefficients and respective activation energies that have been reported in literature.[6, 24, 26, 29, 30, 32, 33, 35, 36] Sometimes a distinction between a non-catalyzed and autocatalytic rate coefficient has although been made.[29, 33] Specifically, Cheikh et al.[32] define different activation energies depending on an excess of butanol or phenyl isocyanate (PhNCO), indicating that systematic data are lacking on the elementary reaction level.
In what follows, a kinetic study of the reaction of PhNCO and 1-butanol to form butyl phenyl carbamate (Scheme 6) under a broad range of initial concentrations is presented. A kinetic Monte Carlo model has been developed which accounts for several auto- and reagent catalysis pathways to analyze the experimental data and to assess the values of the kinetic rate coefficients at different temperatures. It will be shown that alcohol, isocyanate and urethane catalysis need to be addressed to describe the kinetics of urethane formation in a more fundamental manner.

Materials and Methods

For the kinetic experiments, phenyl isocyanate (PhNCO; ≥98%) and 1-butanol (1-BuOH; 99.9%) were used as obtained from Aldrich. 1-Butanol was dried over 3A° molecular sieves. Dichloromethane (DCM; 99.8+%, amylene stabilized, Aldrich) was used as the solvent. For quenching the reaction at various yields, tert-butyl amine (≥ 99.5%, Aldrich) was used. 1,2-Dichloroethane (DCE; anhydrous, 99.8%, Aldrich) was used as internal standard. The butyl-phenyl carbamate (BPC) product was produced for signal identification purposes by reaction of 0.5 ml 1-BuOH with an equimolar amount of PhNCO in 0.5 ml DCM. After complete reaction DCM was evaporated.
The purity of the carbamate product was verified by $_1$H-NMR measurements performing dilution in deuterated chloroform ($CDCl_3$; 99.8%, Euriso-top) and using Bruker 300 MHz equipment, as well as by gas chromatography (GC), using a Thermo Scientific Trace GC Ultra occupied with an Agilent HP 5 column. Hydrogen (H_2) was used as the carrier gas with a flow rate of 1.5 ml min^{-1}. The initial temperature was 223 K and kept constant for 3 minutes. The temperature was then gradually increased to 573 K at a rate of 60 K min^{-1}. The final temperature was kept constant for 4 min (spectra: Figure S1 and S2 of the Supplementary Information). The carbamate was also added in the reaction mixtures with the goal of studying the autocatalytic effect of the product.

Experimental reaction kinetics for quasi stoichiometric ratios of the reactants.

Reactions between phenyl isocyanate and 1-butanol were performed in solutions of 1 ml DCM. The stoichiometric ratios of phenyl isocyanate, 1-butanol and butyl-phenyl carbamate (BPC) were varied as reported in Table 2 to promote reagent- or autocatalytic pathways. Accordingly, the conditions for the quasi-stoichiometric experiments also include measurements with either slight alcohol and isocyanate excess. All reactions were performed at 293 K, 300 K and 303 K.
Samples of 20 µl were taken at regular times while the reaction was proceeding and the aliquots were added to 2 ml vials containing 0.25 mol L^{-1} of t-butyl amine and 0.15 mol L^{-1} of the internal standard, making a total volume of 1 ml. Amine was used to quench PhNCO by forcing it to react with this molecular thereby stopping further reaction with 1-butanol. For the samples containing higher initial PhNCO concentrations, 0.60 mol L^{-1} of the amine was added instead of 0.25 to ensure the complete reaction of PhNCO.
The samples were analyzed by GC analysis with the previously described method. The concentration of the reactants and products were determined according to the separately performed calibrations via integration of the corresponding chromatographical peaks.

Table 2: Initial concentrations of 1-BuOH, PhNCO and the carbamate in the reaction mixtures of the kinetic experiments with quasi stoichiometric ratios of the reactants.

Initial molar ratio/concentration BuOH:PhNCO:BPC	BuOH [mol L^{-1}]	PhNCO [mol L^{-1}]	BPC [mol L^{-1}]
1:1:0	$1.86\ 10^{-1}$	$1.83\ 10^{-1}$	0
1.5:1:0	$2.73\ 10^{-1}$	$1.83\ 10^{-1}$	0
2:1:0	$3.72\ 10^{-1}$	$1.83\ 10^{-1}$	0
2.5:1:0	$4.59\ 10^{-1}$	$1.83\ 10^{-1}$	0
1:2:0	$1.86\ 10^{-1}$	$3.66\ 10^{-1}$	0
1:2.5:0	$1.86\ 10^{-1}$	$4.67\ 10^{-1}$	0
1:1:0.25	$1.86\ 10^{-1}$	$1.83\ 10^{-1}$	$4.5\ 10^{-2}$
1:1:0.5	$1.86\ 10^{-1}$	$1.83\ 10^{-1}$	$8.9\ 10^{-2}$
1:1:0.75	$1.86\ 10^{-1}$	$1.83\ 10^{-1}$	$1.34\ 10^{-1}$

Experimental reaction kinetics in the presence of large excess of 1-butanol.

The reactions were performed in volumes of 3 ml with DCM as the solvent, according to the conditions in Table 3, always at 273 K. The concentration of butyl phenyl carbamate was tracked during the reaction by UV-Vis measurements with a Varian Cary 50 Scan UV-Vis spectrophotometer operative at a wavelength of 282 nm.[41, 42].

Table 3: Initial concentrations of 1-BuOH and PhNCO in the reaction mixtures of the kinetic experiments with large excess of 1-butanol. The total volume of the reaction mixture is 3 ml.

Volume 1-butanol [ml]	BuOH [mol L^{-1}]	PhNCO [mol L^{-1}]
1	3.64	$1.51\ 10^{-4}$
1.5	5.46	$1.51\ 10^{-4}$
2	7.29	$1.51\ 10^{-4}$
2.5	9.11	$1.51\ 10^{-4}$

Kinetic modeling: principles and reactions.

Kinetic Monte Carlo (*k*MC) modeling of the PhNCO and 1-BuOH reaction is performed, applying the well-established Gillespie Stochastic Simulation Algorithm (SSA).[43-45] Opposed to the state-of-art, several competitive catalytic pathways are jointly considered. Starting from the reaction pathways presented in Scheme 7, which are mostly based on literature (cf. Scheme 1-5), Table 4 summarizes the reactions accounted for in the kinetic model. DCM was chosen as a kinetically inert polar aprotic solvent to not overcomplicate the kinetic analysis.

The associated rate coefficients at a given temperature have been determined by fitting experimental PBC concentration data as recorded under isothermal conditions. From the so-obtained individual rate coefficients at different temperatures, Arrhenius parameters could then be deduced.

A two-step procedure is applied to minimize the number of reaction pathways considered. In a first step, a basic model containing reaction pathways 1 to 4 from Table 4 is applied to describe the reaction kinetics starting under quasi stoichiometric conditions. In a second step, the reactions 2’ and 2’’ are also accounted for to capture the observed kinetic behavior with large excess of 1-butanol, leading to the introduction of an extended model with 6 reaction pathways (1-4, 2’, and 2”). It can be seen in Scheme 7 that for the complex C (reaction pathway 2’ and 2”) the six membered ring has been proposed over the eight membered ring, since angles of 120° deliver a higher stability to the formed structure. As shown further, the extended model is also appropriate to model kinetics under (quasi)-stoichiometric conditions. In any case, complex formation occurs, which is a highly novel kinetic insight.

Most reactions in Table 4 are catalytic (molecule-assisted) so that the variation of the initial conditions, i.e., from (quasi)-stoichiometric to OH-excess, is indispensable for a solid evaluation of the importance of the respective reaction pathways. To back-up this statement it should be realized that the relation between a given pathways and the product concentration profile is dependent on the reaction pathway. In the absence of catalyst, the product formation rate is expected to follow a second-order rate law. For a third-order alcohol (reactant) catalysis according, a more pronounced decrease in formation rate is likely observed with increasing conversion (alcohol consumption). In carbamate (product/auto) catalysis, at least, a less pronounced decrease rate is to be expected towards increasing conversion.

1. non-catalyzed reaction

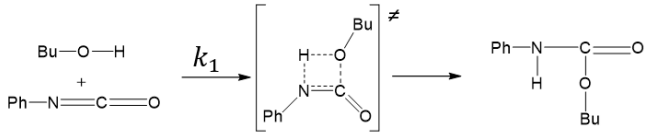

2. alcohol catalysis

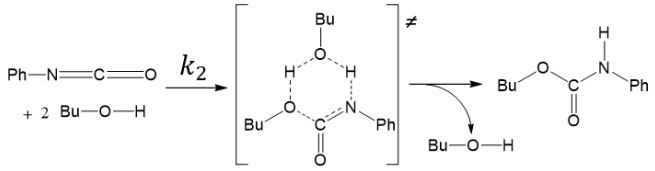

2' and 2". additional alcohol catalyzed pathway

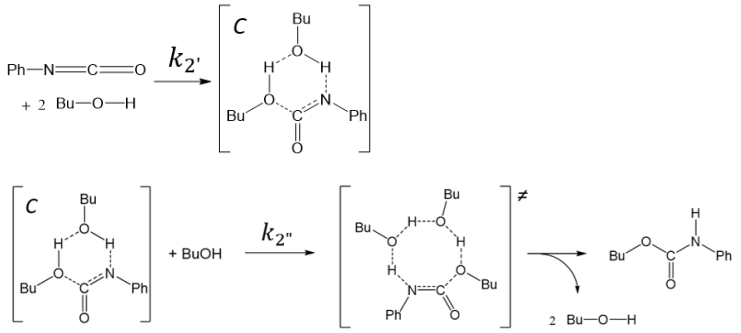

3. isocyanate catalysis

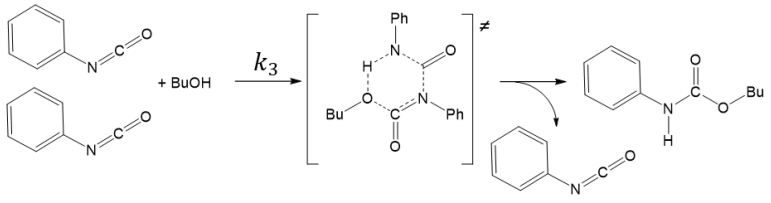

4. carbamate (auto-)catalysis

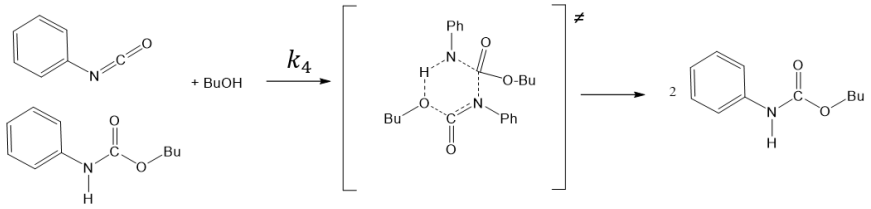

Scheme 7: Reaction pathways in the presented kinetic model for the phenyl isocyanate and 1-butanol reaction. The basic model only employs reaction 1, 2, 3 and 4, whereas the extended model also contains the two-step reaction defined by 2' and 2" with C being a complex; note that in 2 it is assumed as the transition state.

Table 4: Reaction pathways for the phenyl isocyanate and 1-butanol reaction accounted for in the kinetic model. The basic model employs reaction 1, 2, 3 and 4, whereas the extended model also contains the two-step reaction defined by 2' and 2" with C indicating a preactivated complex (complementary to Figure 7).

Type of reaction pathway	**Equation**	***k***
1. *non-catalyzed reaction*	$PhNCO+BuOH \rightarrow BPC$	k_1
2. alcohol catalysis	$PhNCO+2\ BuOH \rightarrow BPC+BuOH$	k_2
2'. alcohol catalysis (i)	$PhNCO+2\ BuOH \rightarrow C$	$k_{2'}$
2''.alcohol catalysis (ii)	$C+BuOH \rightarrow BPC+2\ BuOH$	$k_{2''}$
3. isocyanate catalysis	$2\ PhNCO+BuOH \rightarrow BPC+PhNCO$	k_3

4. urethane catalysis $PhNCO+BuOH+BPC \rightarrow 2\ BPC$ k_4

Results and Discussion

Model sensitivity analyses are in a first phase conducted at 293 K for both the basic and the extended model to better understand why the six rate coefficients (*k* values) in Table 4 are needed to grasp the kinetics under a broad range of conditions. The central values for these sensitivity analyses (1· *k*) are the final values as obtained by tuning to experimental data and are displayed in Table 5. A single rate coefficient is always varied in the sensitivity analysis from 0.1· *k* to 10 · *k* while keeping the residual parameters constant. In a second phase, Arrhenius parameters are derived by also considering experimental data at 300 and 303 K. It will be further highlighted that both models are complementary so that practically only the extended model can be employed. The kinetic interpretations are supported by reaction probability analysis.

Table 5: Rate coefficients as tuned for both models at 293 K; the extended model parameters can describe both the experimental data with quasi stoichiometric conditions and a large initial excess of alcohol. The values in this table are the central values for the sensitivity analyses.

k **[L mol^{-1} s^{-1}] or [L^2 mol^{-2} s^{-1}]**	**Basic model**	**Extended model**
k_1	1.0 10^{-5}	1.0 10^{-5}
k_2	4.0 10^{-4}	4.0 10^{-4}
$k_{2'}$	-	3.0 10^{-3}
$k_{2''}$	-	5.0 10^{-4}
k_3	7.5 10^{-6}	7.5 10^{-6}
k_4	1.2 10^{-3}	1.2 10^{-3}

Model sensitivity analyses for basic and extended model.

Focusing on the concentration time variation of the BPC product, model sensitivity analyses have been carried out for each rate coefficient, while keeping the other reaction coefficients constant. This is done first for the basic model (k_1, k_2, k_3, and k_4) and subsequently for the extra reactions in the extended model ($k_{2'}$ and $k_{2''}$). Each rate coefficient was varied over a range with as boundaries 0.1. *k* and 10 . *k.*

For the basic model, the sensitivity analyses (results in Figure 1-4) have been done for a stoichiometric ratio of PhNCO and 1-BuOH, employing an initial concentration of 1.8 10^{-1} mol L^{-1} each. In Figure 1a, the sensitivity analysis of the non-catalyzed reaction between the isocyanate and the alcohol in the basic model is presented (k_1 variation). It can be seen that a decreasing factor 2 or 10, and an increasing factor 2 do not affect the modeling results in a very significant way, as the bottom 4 lines are very close to each other. However, an increase by a factor 10 (upper line) increases the overall reaction rate to a large extent. Hence, to reliably determine a non-catalytic pathway rate coefficient (assuming competitive reactions) one likely needs a system with a sufficiently high k_1.

Figure 1b shows the sensitivity analysis of the alcohol catalyzed reaction (k_2 variation). It follows that a change of k_2 has a major influence on the concentration-time dependency. An increased relevance of the alcohol catalysis route leads to a steeper curve at low reaction times, and a flattening of the curve at the higher reaction times. This can be explained by the higher probability of a transition state formed by two alcohol molecules and one isocyanate molecule at the beginning of the reaction compared to the end.

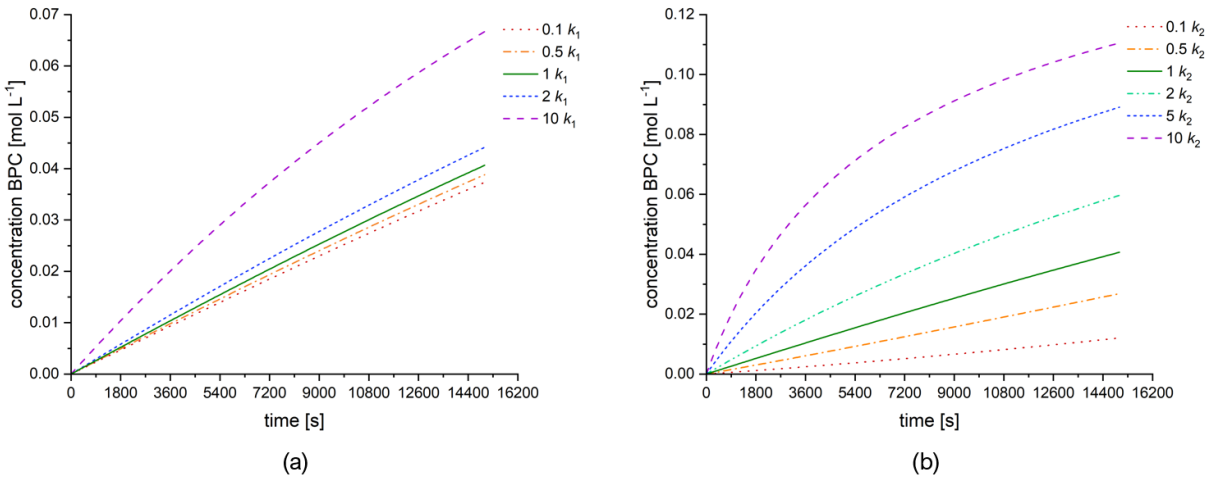

Fig. 1: Model sensitivity analysis for the product concentration variation towards a change in rate coefficient for (a) the non-catalyzed (reaction 1 in Table 4) and (b) the alcohol catalyzed reaction (reaction 2 in Table 4) between PhNCO and BuOH. Respective reference rate coefficients, *k* values, in Table 5 at 293 K.

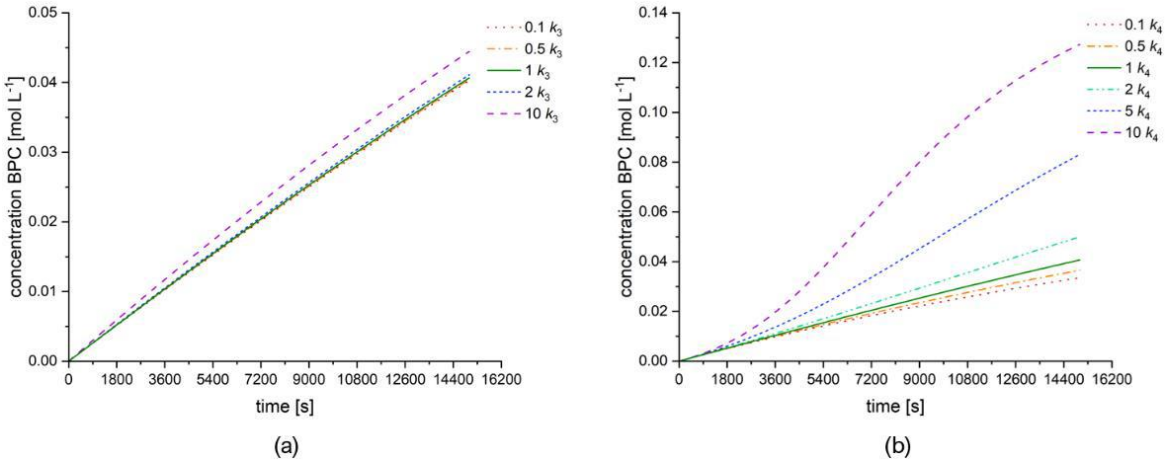

Fig. 2: Model sensitivity analysis towards a change in the rate coefficient for (a) the isocyanate catalyzed reaction between PhNCO and BuOH (reaction 3 in Table 4) and (b) the urethane catalyzed reaction between PhNCO and BuOH (reaction 4 in Table 4). Respective reference rate coefficients, *k* values, in Table 5 at 293 K.

In Figure 2a, the sensitivity analysis for the isocyanate catalysis reaction is presented (k_3 variation). It can be concluded that a change of k_3 by a factor up to 10 has a minor influence with always a quite straight line close to the reference simulation results, and even negligible changes for the selected cases with decreased k_3. One could thus at first sight remove this reaction from the kinetic model. However, as illustrated below, at higher temperatures this reaction gains importance, e.g., the relative increase in k_3 will be higher than for k_2. Hence, the kinetic model is in general more representative in case reaction 3 in Table 4 is taken into account. The corresponding sensitivity analysis with respect to the tuned k_3 at 303 K, and at 293 K with a 2 times excess of PhNCO, can be found in Figure S3 of the Supplementary Information.

Figure 2b shows the sensitivity analysis for the urethane catalysis (k_4). Increasing k_4 leads to a major effect on the product formation rate. Specifically, starting from a multiplication of the rate coefficient by a factor 5, a clear sigmoidal curve can be observed. In other words, a threshold formation of urethane groups leads to a sufficient (auto-)catalytic effect, enhancing the further formation of the reaction product. Although the reference value for k_4 is quite high (Table 5), no sigmoidal shape is observed in the experiments (cf. the straight line shape of the green line in Figure 2b). This can be explained by the pronounced parallel alcohol catalysis (high k_2 value), which manifests itself very pronouncedly in the beginning of the reaction, while the effect of urethane catalysis is only once the product yield increases.

This competitive kinetic effect is highlighted in bar format in Figure 3, displaying the 4 reaction probabilities for the basic model at 7 reaction times. The green bars (alcohol catalysis) are always dominant, but a more similar contribution becomes evident at higher reaction times via the red bars (carbamate catalysis). At any time, the

non-catalyzed pathway contributes to a low but not a negligible degree. Note that a more pronounced non-catalyzed pathway (higher k_1 in Figure 1a) leads to a concentration time dependency more typical for an overall second order reaction, first order in each reactant. The reactions 2-4 however mask such dependency, explaining the large scatter in (effective) kinetic parameters in Table 1.

For the extended model, focusing only on the variation of $k_{2'}$ and $k_{2''}$, a sensitivity analysis has been performed of which the main results are presented in Figure 4, considering a large excess of butanol: initial BuOH concentration of 3.64 mol L^{-1} vs. 1.51 10^{-4} mol L^{-1} initial concentration of PhNCO. The reference values of $k_{2'}$ and $k_{2''}$ in Table 5 are again the tuned ones and based on UV-Vis experiments. It can be seen in Figure 4a that $k_{2'}$ is decisive for the initial slope of the concentration curve, with a lower value leading to a steeper increase. Figure 4b displays in turn that $k_{2''}$ influences the reaction rate at higher conversion, once a significant amount of complex is formed.

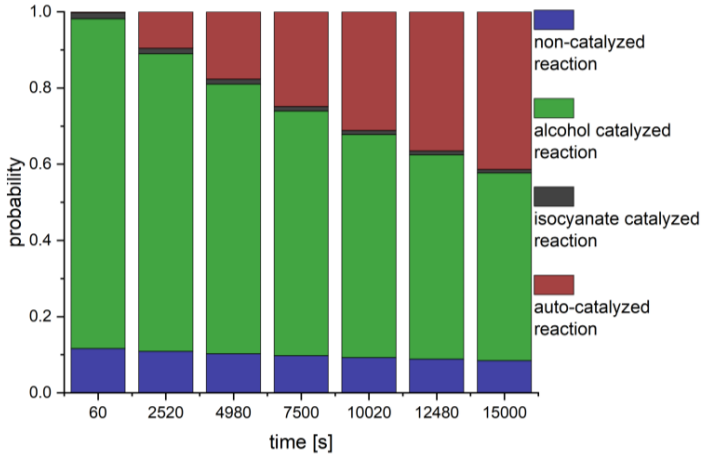

Fig. 3: Probabilities of the reactions 1, 2, 3 and 4 in Table 4 at 7 reaction times, according to the values in Table 5 at 293 K and employing an initial concentration of 1.8 10^{-1} mol L^{-1} for both 1-BuOH and PhNCO. For the reference (tuned) parameters in this table the alcohol catalysis (green bar) is always dominant but at higher reaction times the contribution of the carbamate catalysis is very similar in importance. Line plot as Supplementary Figure S4 (303 K result as Supplementary Figure S5).

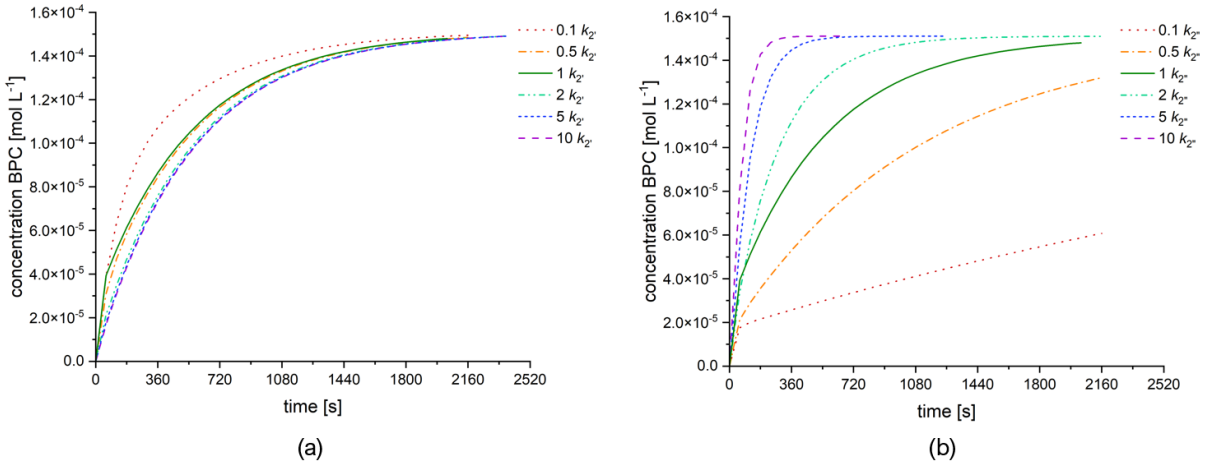

Fig. 4: Sensitivity of the extended model (besides k_1, k_2, k_3 and k_4, $k_{2'}$ and $k_{2''}$ are also included) towards a change in rate coefficient for the two-step alcohol catalyzed reaction with an 8 centered transition state between PhNCO and BuOH at large alcohol concentrations: (a) $k_{2'}$ and (b) $k_{2''}$ (reaction 2' and 2'' in Table 4).

Kinetic analysis under (quasi) stoichiometric conditions.

For the kinetic modeling with no or only small excess of 1-BuOH one could put forward that reaction 2' (and 2'') in Table 4 can be removed from the overall reaction scheme (Scheme 7). As diluted solutions are considered and the initial concentration of butanol is relatively low, the rate for the reaction pathway of 2 alcohol molecules and

one PhNCO is at first sight expected to have a very low probability. One would expect the need of a very high rate coefficient to make a trimolecular reaction very important under diluted conditions, justifying this approach. Figure 5 shows the fitted BPC concentration profile at 293 K. The deduced rate coefficients are presented in the second column of Table 6, which are the same as in the second column of Table 5 being the central values of the sensitivity analysis, as explained before. Similar comparisons at 300 K and 303 K are presented in Figure S6 of the Supplementary Information, with the rate coefficients shown in the third and fourth column of Table 6. Overall, an acceptable agreement is obtained between experiment and model at the three reaction temperatures. From the orders of magnitude of the rate coefficients in Table 6, it can be derived that the autocatalysis and butanol catalysis routes are the main paths in the reaction scheme, making hydrogen bond induced activation relevant for urethanization. Both pathways display nominal values of ca. 10^{-3} and 10^{-4} respectively, while the non-catalyzed and isocyanate catalyzed path are only characterized by a nominal value of ca. 10^{-5}. A zero value for the latter two pathways results in small changes so that at least a certain sensitivity toward parameter tuning could be claimed based on the selected set of experimental data. Note that highly diluted conditions and systems with high NCO excess, as in the case of some commercially available NCO-terminated prepolymers, could although still imply classical second-order behavior.

Based on rate coefficients per temperature in Table 6, Arrhenius plots can be made for each rate coefficient as presented in Figure 6. The corresponding values for the pre-exponential factor A and the activation energy E_a are mentioned in the last two columns in Table 6. It follows that the butanol catalyzed reaction is the least activated with an E_a of 8.7 kJ mol^{-1}, whereas the carbamate catalyzed reaction is the most activated with an E_a of 58.7 kJ mol^{-1}. The non-catalyzed reaction and the isocyanate catalyzed reaction are still rather activated with an E_a of 46.8 and 36.3 kJ mol^{-1}, respectively.

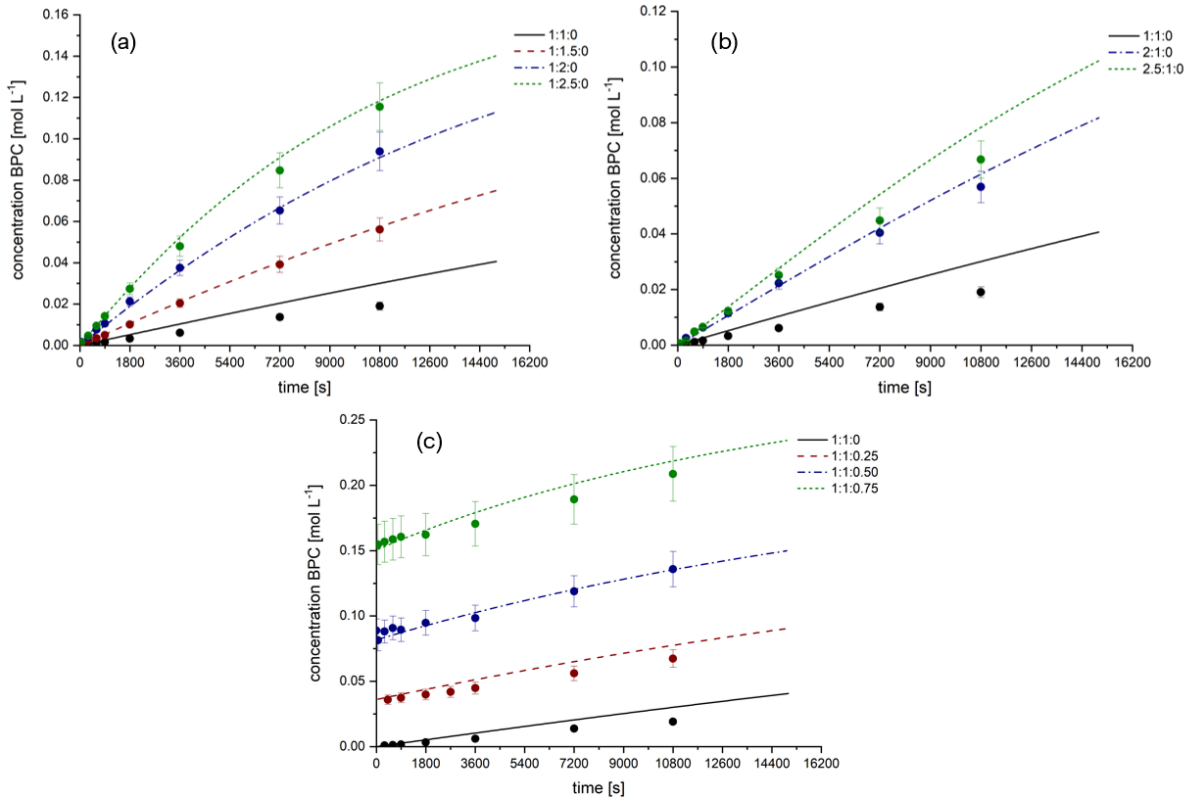

Fig. 5: Experimental (●) and modelling (-) data for variable initial butanol concentrations (a), variable initial PhNCO concentrations (b), and variable initial carbamate concentrations (c) at 293 K. In all cases quasi stoichiometric conditions according to Table 2. Analogue figures for 300 K and 303 K in the Supplementary Information.

Table 6*:* Tuned (reference) rate coefficients for the first four reactions in Table 4 at 293 K, 300 K, and 303 K, as well as the corresponding Arrhenius parameters (Figure 6), obtained from the fit with the experimental data presented in Fig. 5 and S6; all experiments performed with low initial concentrations for all reactants.

	293K	300 K	303 K	*A [L mol-1 s-1]* or [L_2 mol^{-2} s^{-1}]	*Ea* [kJ mol-1]
k_1 *[L* mol^{-1} *s-1]*	1.0 10^{-5}	1.3 10^{-4}	2.0 10^{-5}	2.09 10^{3}	46.8 ± 18.3
k_2 *[L2* mol^{-2} *s-1]*	4.0 10^{-4}	4.4 10^{-4}	4.5 10^{-4}	1.43 10^{-2}	8.7 ± 0.0
k_3 *[L2* mol^{-2} *s-1]*	7.5 10^{-6}	1.0 10^{-5}	1.3 10^{-5}	2.18 10^{1}	36.3 ± 5.9
k_4 *[L2* mol^{-2} s^{-1}*]*	1.2 10^{-3}	2.0 10^{-3}	2.7 10^{-3}	3.39 10^{7}	58.7 ± 5.0

Upon comparing the tuned rate coefficients in Table 6 with those from literature (Table 1), it follows that they are of the same order of magnitude (nominal) for the autocatalyzed and butanol catalyzed route (reaction 4 and reaction 2 in Table 4), which have shown to be the most probable pathways in the present work (largest bars in Figure 3). Also, the activation energies described in literature (Table 1) are comparable with the values in Table 6. A more detailed comparison is although non-trivial, as the focus in literature has been mainly on obtaining overall effective rate coefficients for the urethane formation, thus kinetic parameters lumped over several competitive mechanisms. Studies on the catalytic effects mainly focused on confirming an autocatalytic or an alcohol catalyzed pathway, without really determining rate coefficients for each reaction pathway specifically. Furthermore, the use of different solvents in previous research has an additional effect on the parameter determination and comparison because hydrogen-bonds and polarity effects likely impact the reaction probabilities [14, 17, 26, 27, 30, 31, 46, 47]. In the present work, the used (aprotic) solvent DCM, which has a dielectric constant of 9, features no ability of donating hydrogen bonds [48], and is immiscible with water [49].
It should be reminded that almost no activation energies have been reported for urethane formation at the provided elementary reaction level, highlighting the relevance of Figure 6. For the first time Arrhenius plots for key reactions are displayed relevant for a step-growth PU synthesis to a level as quite standard for chain growth polymerization [50-52]. By decoupling the full reaction scheme and defining rate coefficients for each pathway, a gap has been diminished in the field of PU kinetics.

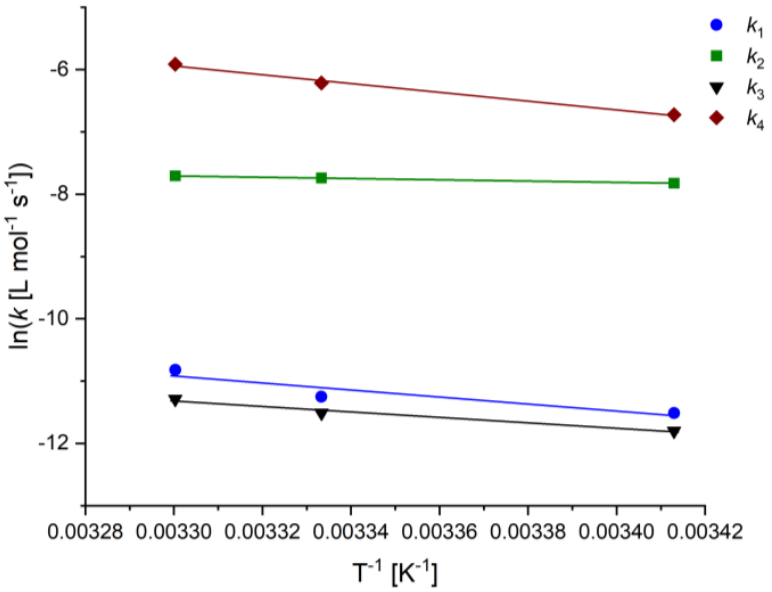

Fig. 6: Arrhenius plot for the rate coefficients based on the data in Table 6 (tuning of conditions with the basic model).

Kinetic analysis under large excesses of 1-butanol.
Figure 7 shows the experimental data as recorded with UV-Vis spectroscopy (example spectra: see Supplementary Information S7) as well as the simulation results as obtained with the basic model (dashed lines) for the reaction conducted with a high 1-BuOH excess. Surprisingly, following conventional kinetic insights, the basic model predicts a way too fast reaction. In other words, the experimental rate (black points) is lower and the simulated rate lower than for the quasi-stoichiometric case, although the content of the catalytic species, i.e., 1-BuOH, was significantly increased. The extended model is therefore needed, as confirmed by the solid lines in Figure 7, which are obtained by only tuning the coefficients $k_{2'}$ and $k_{2''}$ while keeping the residual parameters at the values as found by the basic model at quasi stoichiometric conditions (see last column of Table 5).

This much better description with the extended model highlights a kinetic relevance of the complex C in Scheme 7. For a general kinetic description, it is thus very relevant to take into account the complex formation consisting of 2 butanol molecules and 1 PhNCO molecule, enabling the formation of the 8 membered transition state that was introduced by Gertig et al. [14].

This is further confirmed in Figure 8, showing in subplot (a) the concentrations trajectories of the isocyanate, the product, and C for the extended model, in subplot (b) additionally the concentrations for the former two in the basic model, and in subplot (c) the reaction probabilities at 7 times for the extended model. It follows from Figure 8a that for the k_2 and k_2'' values reported in Table 5, the C concentration increases rapidly at the expense of the free OH. The consequence is a dominance of the reaction path 2'' over almost the entire course of the reaction (light green bar), as can be seen in subplot (c) of Figure 8 (line plot in Figure S8 of the Supplementary Information). Only at the beginning of the reaction, a significant but rapidly decreasing contribution of OH catalysis via reaction path 2 is predicted (dark green bar). Consequently, reaction pathways 1, 2, 3 and even 4 are suppressed almost completely, resulting in a retardation (black dashed vs black full line in Figure 8b).

A next logical step is to verify whether the generalized model with 6 reaction pathways also works for the previously studied quasi stoichiometric conditions. Figure 9a shows that the extended model performs well, selecting a 1:2:0 experimental condition from Table 2 at 293 K. Figure 9b (line plot in Figure S9 of the Supplementary Information) highlights that the absolute values of the reaction probabilities are different compared to the basic model (Figure 3). The complex formation is dominant but on a relative basis it again follows that the non-catalyzed reaction pathway (blue bars) possesses a very minor importance, and the conventional alcohol catalyzed pathways loses in relevance compared to the auto-catalytic one (red bars) at higher reaction times. The reaction between C and a 1-butanol molecule (k_2'') is in any situation sufficiently fast to compensate for the lower concentrations of isocyanate and 1- butanol due to complex formation, slowing down reaction pathways 1 to 4.

Notably the balance in alcohol and isocyanate molecules is maintained in both models, bearing in mind that one complex molecule contains one phenyl isocyanate and two one-butanol molecules. This is made clear in Figure 9c and Figure 9d, displaying coinciding lines for the phenyl isocyanate concentration (basic model) and the concentration of phenyl isocyanate lumped with complex (extended model) as well coinciding lines for the 1-butanol concentration (basic model) and the concentration of 1-butanol lumped with twice the complex. Hence, the proposed mechanism with the complex C is consistent with experimental data in the field showing consistent net rates for the isocyanate and the carbamate under diluted conditions. In other words, the current work puts forward that certain experimental data recording should be seen in lumped format, at least in case there is insufficient sensitivity difference between isolated isocyanate, isolated alcohol and complexes.

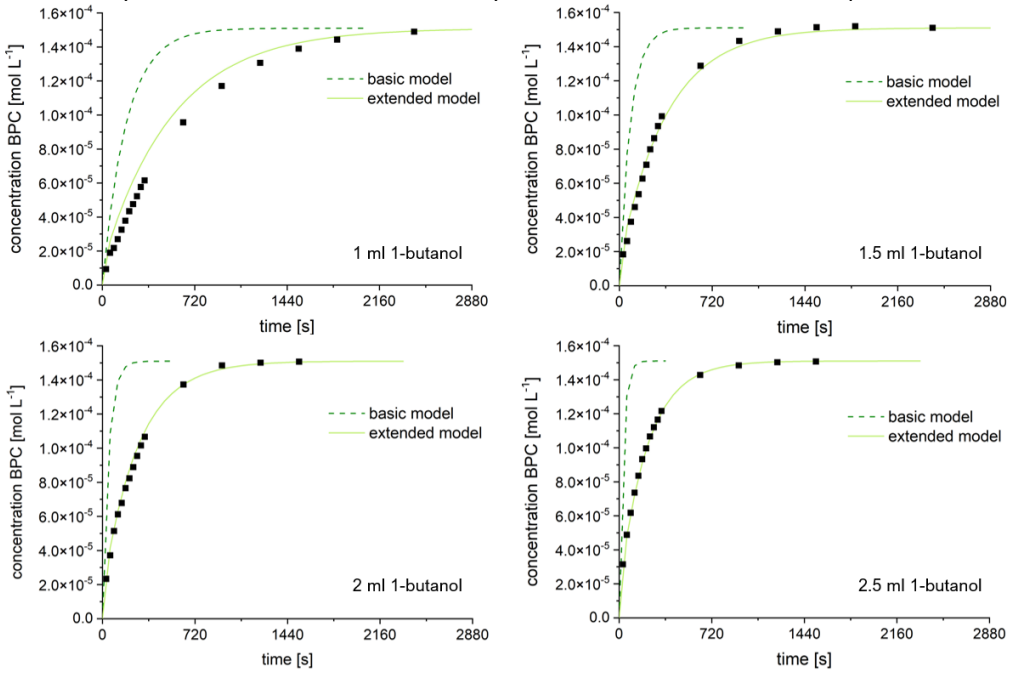

Fig. 7: Experimental (□) data with a large excesses of 1-butanol at 293 K as well as the modeling data with the basic (- -) and extended (-) model (parameters in Table 5). Only extra tuning of k_2' and k_2".

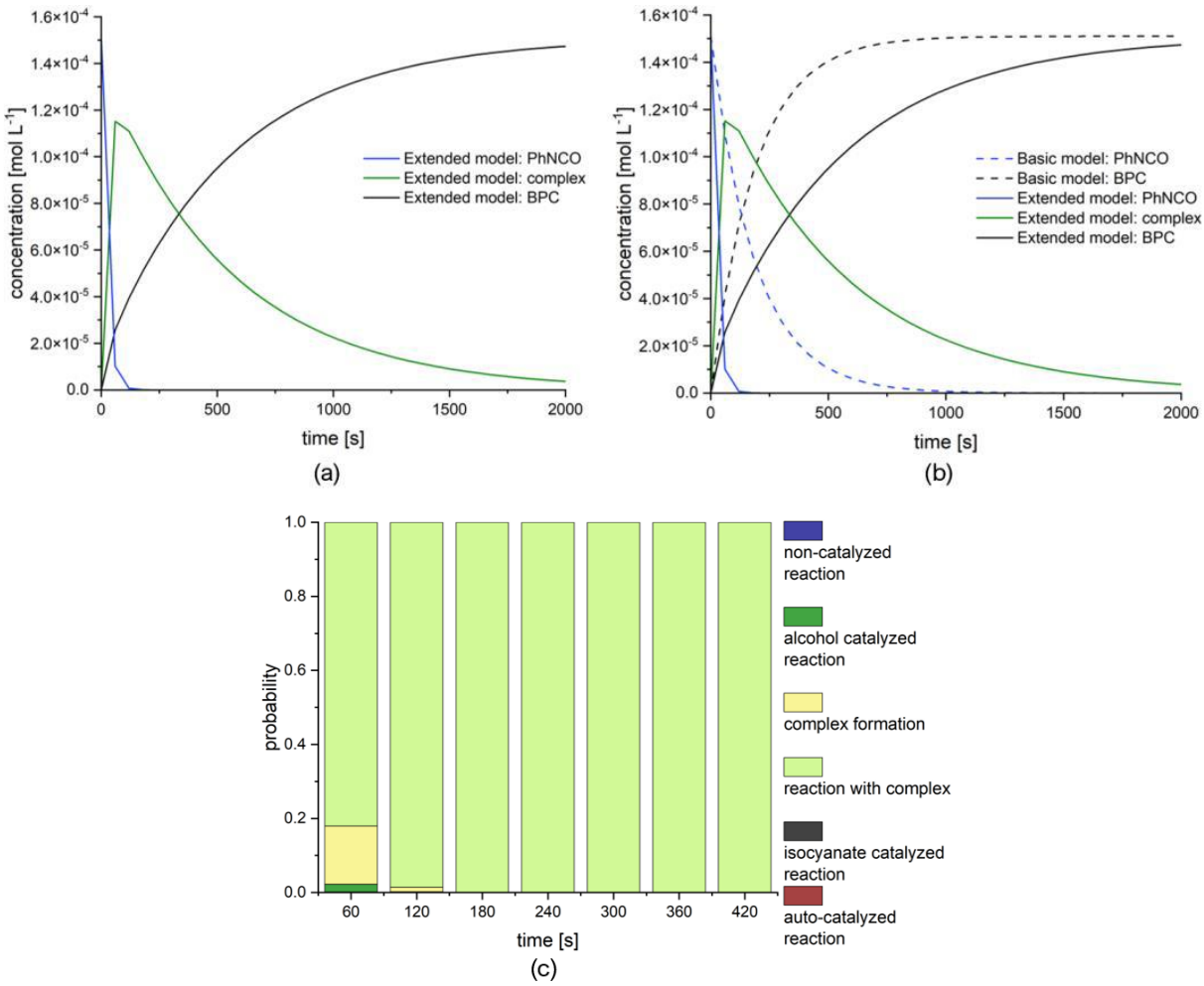

Fig. 8: (a) Concentrations of PhNCO, the complex C, and BPC modelled by the extended model (BuOH initial concentration of 3.64 mol L^{-1} and PhNCO initial concentration of 1.51 10^{-4} mol L^{-1})(b) Update of subplot (a) with basic model concentrations for PhNCO and BPC (c) probabilities of the reactions in Table 4 (extended model) at 7 reaction times; parameters values in Table 5 at 293 K.

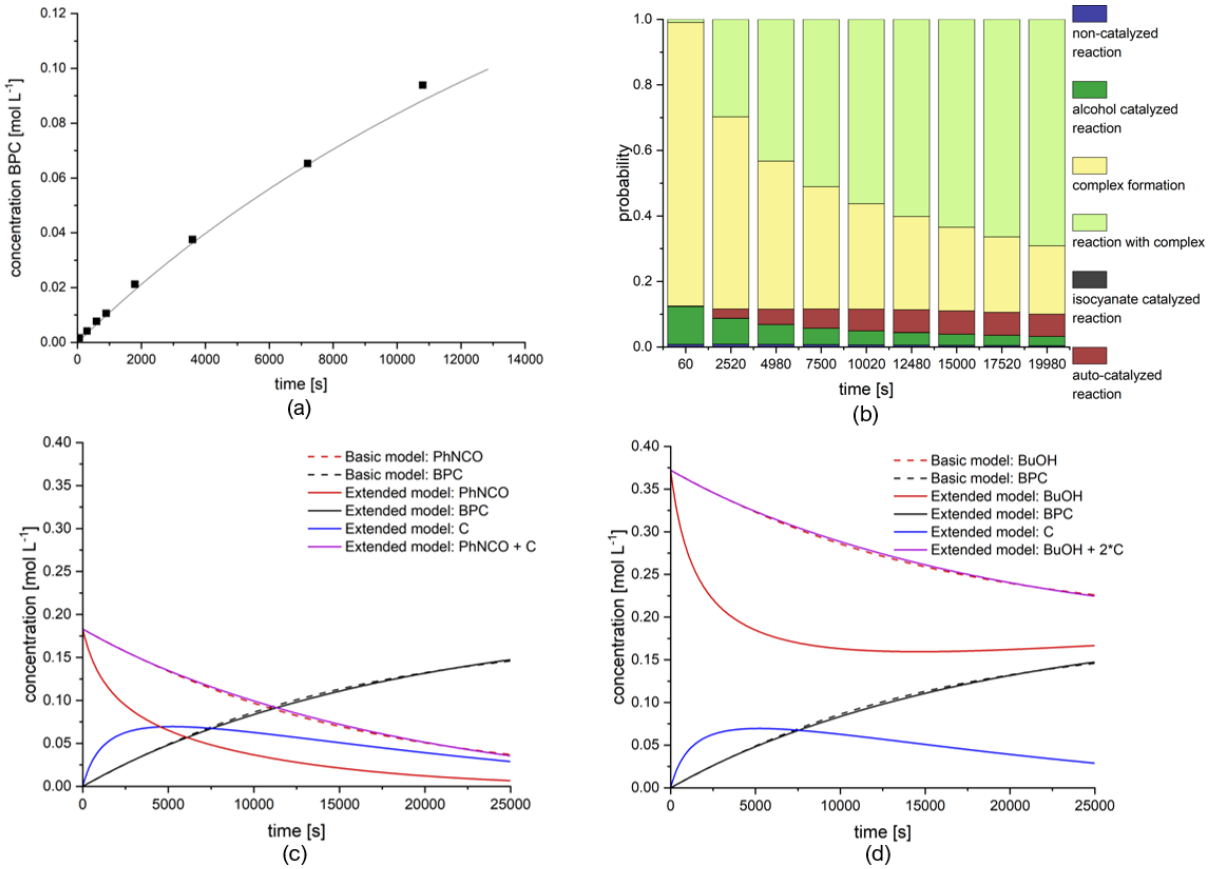

Fig. 9: (a) Experimental (□) and extended model (-) data for the 1:2:0 experiment in Table 2 (low reactant concentrations: initial BuOH concentration of 3.72 10^{-1} mol L^{-1} and an initial PhNCO concentration of 1.83 10^{-1} mol L^{-1}, 293 K; rate coefficients in the second column of Table 5). (b) Reaction probabilities from the extended model (c) and (d) Comparisons of selected concentrations for phenyl isocyanate, butanol and carbamate as well as balances for isocyanate and alcohol moieties (both the basic and extended model give the same result).

Conclusions

In this kinetic study, the catalytic or molecule assisted pathways for the reaction of 1-butanol and phenyl isocyanate towards butyl phenyl carbamate have been investigated in dichloromethane. This has been done both under quasi stoichiometric reactant concentrations and with large excess of 1-butanol. Experimental data has been fitted with a kinetic Monte Carlo model to determine rate coefficients for each reaction pathway. The overall kinetic interpretation has been

strongly facilitated by plotting reaction probabilities. It has been shown that next to the basic uncatalyzed reaction between one butanol molecule and one isocyanate molecule, an alcohol catalyzed, an isocyanate catalyzed and an autocatalyzed pathway can affect the total reaction rate. The comparison of two models, one basic and one extended, revealed that in high excess of alcohol, the participation of an eight-centered complex must be taken into account to predict the reaction outcome; a basic model without complex predicts a too fast carbamate formation.

Deeper investigation showed that even under low and quasi stoichiometric concentrations the participation of such eight-centered complex is not negligible. Hence, it can we worthwhile to study more extreme less conventional reaction conditions to test reaction mechanisms, as the consideration of only the diluted conditions would not give experimental sensitivity to the formation of the complex.

Notably a good fit of the experimental data with the basic model can still be obtained at these low initial concentrations. The reaction rate with the complex is still sufficiently fast to compensate for the depletion in isocyanate and alcohol via the complex formation in the extended model so that a basic model without such depletions formally gives similar simulation results.

The reported set of rate coefficients opens the door to obtain Arrhenius parameters more on the elementary reaction level for polyurethane synthesis, closing the gap between step- and chain-growth polymerization regarding kinetic parameter libraries currently only containing (reaction condition dependent) effective rate

coefficients. Future work will be directed to the implementation of the impact of the solvent type and the substitution degree inside the model. It is also worthwhile to investigate the impact of a deliberately added catalyst Furthermore, the relevance of additional side reactions will be explored.

Conflicts of interest

There are no conflicts to declare.

Acknowledgements

L.T. acknowledges the Research Foundation—Flanders via a Scholarship: FWO.SPB.2021.0036.01. L.T., M.E., P.S. and D.R.D. are grateful to BASF SE for support and open discussions.

References

1. M. Szycher, *Polyurethanes*, CRC press Boca Raton, 2013.
2. G. Wegener, M. Brandt, L. Duda, J. Hofmann, B. Klesczewski, D. Koch, R.-J. Kumpf, H. Orzesek, H.-G. Pirkl and C. Six, *Applied Catalysis A: General*, 2001, **221**, 303-335.
3. E. Sharmin and F. Zafar, *Polyurethane*, 2012, 3-16.
4. H. Somarathna, S. Raman, D. Mohotti, A. Mutalib and K. Badri, *Construction and Building Materials*, 2018, **190**, 995-1014.
5. A. Eceiza, J. Zabala, J. Egiburu, M. Corcuera, I. Mondragon and J. Pascault, *European polymer journal*, 1999, **35**, 1949-1958.
6. E. Delebecq, J.-P. Pascault, B. Boutevin and F. Ganachaud, *Chemical reviews*, 2013, **113**, 80-118.
7. M. Szycher, *Journal of biomaterials applications*, 1988, **3**, 297-402.
8. K.-K. Tremblay-Parrado and L. Avérous, *European Polymer Journal*, 2020, **135**, 109840.
9. P. Storozhenko, K. Magdeev, A. Grachev, N. Kirilina and V. Shiryaev, *Catalysis in Industry*, 2020, **12**, 304-315.
10. A. Eceiza, K. De La Caba, G. Kortaberria, N. Gabilondo, C. Marieta, M. Corcuera and I. Mondragon, *European polymer journal*, 2005, **41**, 3051-3059.
11. P. Furtwengler and L. Avérous, *Polymer Chemistry*, 2018, **9**, 4258-4287.
12. A. Tardy, N. Gil, C. M. Plummer, D. Siri, D. Gigmes, C. Lefay and Y. Guillaneuf, *Angewandte Chemie*, 2020, **132**, 14625-14634.
13. M. H. Tran and E. Y. Lee, *Environmental Chemistry Letters*, 2023, 1-25.
14. C. Gertig, E. Erdkamp, A. Ernst, C. Hemprich, L. C. Kröger, J. Langanke, A. Bardow and K. Leonhard, *ChemistryOpen*, 2021, **10**, 534-544.
15. P. K. Maji and A. K. Bhowmick, *Journal of Polymer Science Part A: Polymer Chemistry*, 2009, **47**, 731-745.
16. M. Zajac, H. Kahl, B. Schade, T. Rödel, M. Dionisio and M. Beiner, *Polymer*, 2017, **111**, 83-90.
17. H. Sardon, A. Pascual, D. Mecerreyes, D. Taton, H. Cramail and J. L. Hedrick, *Macromolecules*, 2015, **48**, 3153-3165.
18. S. J. Moravek and R. F. Storey, *Journal of applied polymer science*, 2008, **109**, 3101-3107.
19. T. N. M. Tuan Ismail, K. D. Poo Palam, Z. B. Abu Bakar, H. S. Soi, Y. S. Kian, H. Abu Hassan, C. Schiffman, A. Sendijarevic, V. Sendijarevic and I. Sendijarevic, *Journal of Applied Polymer Science*, 2016, **133**.
20. M. R. Di Caprio, C. Brondi, E. Di Maio, T. Mosciatti, S. Cavalca, V. Parenti, S. Iannace, G. Mensitieri and P. Musto, *European Polymer Journal*, 2019, **115**, 364-374.
21. A. L. Silva, *Catalysis reviews*, 2004, **46**, 31-51.
22. X. Y. Huang, W. Yu and C. S. P. Sung, *Macromolecules*, 1990, **23**, 390-398.
23. S. Boufi, M. N. Belgacem, J. Quillerou and A. Gandini, *Macromolecules*, 1993, **26**, 6706-6717.
24. L. Thiele, *Acta Polymerica*, 1979, **30**, 323-342.
25. J. W. Baker and J. Gaunt, *Journal of the Chemical Society (Resumed)*, 1949, 9-18.
26. S. Ephraim, A. Woodward and R. Mesrobian, *Journal of the American Chemical Society*, 1958, **80**, 1326-1328.
27. A.-C. Draye, D. Tarasov and J.-J. Tondeur, *Reaction Kinetics and Catalysis Letters*, 1999, **66**, 199-204.
28. M. Majid, B. Paul, I. Rahman and M. H. Uddin, *Bulletin of Pure and Applied Sciences. Vol. 22C (No. 2)*, 2003, 59-68.
29. B. F. d'Arlas, L. Rueda, P. M. Stefani, K. De la Caba, I. Mondragon and A. Eceiza, *Thermochimica Acta*, 2007, **459**, 94-103.
30. T. Nagy, B. Antal, K. Czifrák, I. Papp, J. Karger-Kocsis, M. Zsuga and S. Kéki, *Journal of Applied Polymer Science*, 2015, **132**.
31. J. W. Baker and J. Gaunt, *Journal of the Chemical Society (Resumed)*, 1949, 19-24.
32. W. Cheikh, Z. B. Rózsa, C. O. Camacho López, P. Mizsey, B. Viskolcz, M. Szőri and Z. Fejes, *Polymers*, 2019, **11**, 1543.
33. A. Y. Samuilov and Y. D. Samuilov, *Russian Journal of Organic Chemistry*, 2018, **54**, 1749-1753.
34. L. Weisfeld, *Journal of Applied Polymer Science*, 1961, **5**, 424-427.
35. P. Król and J. Wojturska, *Journal of applied polymer science*, 2003, **88**, 327-336.
36. J. Peyrton, C. Chambaretaud and L. Avérous, *Molecules*, 2019, **24**, 4332.
37. P. Król, *Journal of applied polymer science*, 1998, **69**, 169-181.
38. E. Vivaldo-Lima, G. Luna-Bárcenas, A. Flores-Tlacuahuac, M. A. Cruz and O. Manero, *Industrial & engineering chemistry research*, 2002, **41**, 5207-5219.
39. D. R. Miller and C. Sarmoria, *Polymer Engineering & Science*, 1998, **38**, 535-557.

40. C. Sarmoria and D. Miller, *Computational and Theoretical Polymer Science*, 2001, **11**, 113-127.
41. H. Buchenauer, L. V. Edgington and F. Grossmann, *Pesticide Science*, 1973, **4**, 343-348.
42. J. F. Cameron and J. M. Frechet, *The Journal of Organic Chemistry*, 1990, **55**, 5919-5922.
43. A. D. Trigilio, Y. W. Marien, P. H. Van Steenberge and D. R. D'hooge, *Industrial & Engineering Chemistry Research*, 2020, **59**, 18357-18386.
44. D. T. Gillespie, *Journal of computational physics*, 1976, **22**, 403-434.
45. D. T. Gillespie, *The journal of physical chemistry*, 1977, **81**, 2340-2361.
46. A. E. Oberth and R. S. Bruenner, *The Journal of Physical Chemistry*, 1968, **72**, 845-855.
47. M. C. Chang and S. A. Chen, *Journal of Polymer Science Part A: Polymer Chemistry*, 1987, **25**, 2543-2559.
48. L. X. Dang, *The Journal of chemical physics*, 1999, **110**, 10113-10122.
49. P. Clapés, P. Adlercreutz and B. Mattiasson, *Journal of biotechnology*, 1990, **15**, 323-338.
50. A. B. Vir, Y. W. Marien, P. H. Van Steenberge, C. Barner-Kowollik, M.-F. Reyniers, G. B. Marin and D. R. D'hooge, *Polymer Chemistry*, 2019, **10**, 4116-4125.
51. O. Monyatsi, A. N. Nikitin and R. A. Hutchinson, *Macromolecules*, 2014, **47**, 8145-8153.
52. S. Beuermann and M. Buback, *Progress in Polymer Science*, 2002, **27**, 191-254.